NANO LETTERS

Letter

pubs.acs.org/NanoLett

Titin-Based Nanoparticle Tension Sensors Map High-Magnitude Integrin Forces within Focal Adhesions

Kornelia Galior,[†] Yang Liu,[†] Kevin Yehl,[†] Skanda Vivek,[‡] and Khalid Salaita*[,†]

[†]Department of Chemistry, Emory University, 1515 Dickey Drive, Atlanta, Georgia 30322, United States

[‡]Department of Physics, Emory University, 400 Dowman Drive, Atlanta, Georgia 30322, United States

Supporting Information

ABSTRACT: Mechanical forces transmitted through integrin transmembrane receptors play important roles in a variety of cellular processes ranging from cell development to tumorigenesis. Despite the importance of mechanics in integrin function, the magnitude of integrin forces within adhesions remains unclear. Literature suggests a range from 1 to 50 pN, but the upper limit of integrin forces remains unknown. Herein we challenge integrins with the most mechanically stable molecular tension probe, which is comprised of the immunoglobulin 27th (I27) domain of cardiac titin flanked with a fluorophore and gold nanoparticle. Cell experiments show that integrin forces unfold the I27 domain, suggesting that integrin forces exceed ~30−40 pN. The addition of a disulfide bridge within I27 "clamps" the probe and resists mechanical unfolding. Importantly, incubation with a reducing agent initiates SH exchange, thus unclamping I27 at a rate that is dependent on the applied force. By recording the rate of S−S reduction in clamped I27, we infer that integrins apply 110 ± 9 pN within focal adhesions of rat embryonic fibroblasts. The rates of S−S exchange are heterogeneous and integrin subtype-dependent. Nanoparticle titin tension sensors along with kinetic analysis of unfolding demonstrate that a subset of integrins apply tension many fold greater than previously reported.

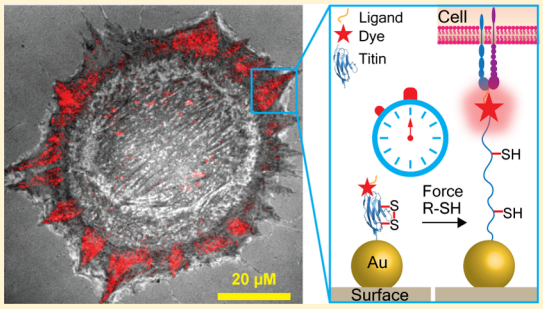

KEYWORDS: *Integrins, mechanotransduction, biophysics, focal adhesion*

Cells adhere to the extracellular matrix (ECM) through transmembrane integrin receptors consisting of an α and β subunit.[1] For example, fibronectin (FN) ECM molecules are primarily recognized by $\alpha_5\beta_1$ and $\alpha_v\beta_3$ integrins that bind the Arg-Gly-Asp (RGD) and Pro-His-Ser-Arg-Asn (PHSRN) motifs.[2] Integrin subtype expression levels are cell type-dependent and dynamic, responding to the chemical and mechanical properties of the ECM.[3] Therefore, determining the magnitude of integrin tension and the spatial and temporal heterogeneity of these forces for different integrin subtypes will help elucidate the role of mechanics in receptor function during cell adhesion and cell migration processes. For example, the existence of heterogeneous distributions of integrin forces within nanoscale domains of a FA is unknown, and it is possible that a subset of integrin receptors experience significant magnitudes of tension that exceed the ensemble average determined by such techniques as traction force microscopy or micropillar array technology.

Integrin activation typically triggers the formation of supramolecular protein assemblies, focal adhesions (FAs), that are comprised of hundreds of different structural and signaling molecules.[4] Collectively, the FA functions to physically and chemically link the cytoskeleton to the ECM.[5] FA assembly/disassembly is highly orchestrated in space and time to accommodate cell polarization and migration activities through inside-out and outside-in signaling mechanisms.[6a,b] While the protein composition of FAs and their dynamics are currently under active investigation, there is limited knowledge about the mechanical forces experienced and transmitted through these structures. For example, except for integrin adhesion receptors[7] and vinculin,[8] to the best of our knowledge, there are no direct measurements of the forces experienced by the hundreds of other proteins making up FAs.

The most common technique to characterize cell adhesion forces is traction force microscopy (TFM), which indicates that forces for adhered fibroblasts range from 1 to 2 nN/μm^2.[9] By estimating the number of bound integrins per unit area (1000 molecules/ μm^2),[10] the force per receptor was also estimated at 1−2 pN per integrin.[9a] However, the challenge with TFM pertains to its limited spatial resolution (~1 μm) and force sensitivity (~nN) because of the cross-linked nature of the polymer. In addition, the deformable TFM substrates influence the cell biology, further convoluting the results.[11]

To address these issues, we pioneered the development of molecular tension fluorescence microscopy (MTFM),[12] which allows for optical imaging of pN-level receptor-mediated forces with high spatial and temporal resolution. MTFM probes consist of an extendable macromolecule such as polyethylene glycol (PEG) or oligonucleotides that are flanked by a fluorophore-quencher pair undergoing resonance energy trans-

Received: September 24, 2015
Revised: November 22, 2015
Published: November 24, 2015

DOI: 10.1021/acs.nanolett.5b03888
Nano Lett. 2016, 16, 341−348

fer (RET). MTFM probes are immobilized onto a substrate and modified with a ligand, such that receptor applied tension extends the linker and dequenches the fluorophore, generating a significant increase in donor emission intensity.

To tailor MTFM probes for integrins, we previously modified PEG_{24} polymer with the cyclic RGDfK peptide and anchored the probe using biotin−streptavidin association.[12f] Fibroblasts cultured on this probe for 45 min caused biotin−streptavidin dissociation, which is surprising because biotin−streptavidin association is often described as the strongest noncovalent bond in nature, suggesting that forces applied by integrins are significant. Nanoparticle-based MTFM probes immobilized using thiol-gold binding, were more mechanically robust and showed that integrin forces exceed 10−15 pN in magnitude.[12d,e] Supporting this result, we and others observed that DNA hairpin tension probes are denatured due to integrin mediated forces, indicating forces in excess of 16 pN.[12c,13] Likewise, tension gauge tether probes, consisting of DNA duplexes decorated with the cRGDfK peptide indicate that integrin activation is associated with peak forces up to ∼50 pN in magnitude.[7] In contrast, Dunn and colleagues determined that integrin-mediated forces are in the range of 1−5 pN based on single molecule imaging of a spidersilk elastin-based tension probe.[14] Therefore, there is discrepancy in the reported integrin forces within FAs.

In this report, we investigate the magnitude of integrin tension within mature FAs by engineering the 27th immunoglobulin domain of cardiac titin (I27), which is structurally and mechanically well-studied both experimentally[15] and through theoretical modeling[16] and displays highly reversible force−extension curves.[17] Based on single molecule force spectroscopy with constant loading rate (0.4 μm/sec), the most probable unfolding force for I27 is significantly greater (∼80−200 pN)[18] when compared to DNA denaturation (∼4−50 pN),[7,12c] and spidersilk elastin extension (∼2−6 pN),[14] and therefore enables the investigation of integrin forces at ranges that are greater than values studied thus far. In principle, the rate of mechanically driven protein/DNA unfolding is exponentially dependent on the applied force, and likewise the cumulative probability of molecular unfolding is also exponentially dependent on the duration of applied force (Supplementary Note 1).[19] Accordingly, this limits the accuracy of inferring a specific magnitude of force from determining the equilibrium distribution of unfolded probes at a given time point. Addressing this limitation, we use the kinetics of titin unfolding rather than the equilibrium distribution of unfolded domains, to more precisely estimate the values of high-magnitude integrin forces within mature FAs and determine the relative contribution of the $\alpha_5\beta_1$ and $\alpha_v\beta_3$ integrins. In principle, this kinetic approach can be used to determine absolute integrin forces at any time point during FA maturation, thus overcoming a longstanding problem associated with the nascent field of molecular tension sensors. Finally, by employing recombinant protein expression this work describes a facile and general approach for engineering of virtually any expressible protein ligand within MTFM probes.

To label the I27 domain with a fluorophore, we initially introduced the acyl carrier protein (ACP)-tag near the N-terminus which can be enzymatically modified at its serine residue with a fluorophore with over 90% yield (Figure 1A).[20] The probe displayed the "GRGDS" motif, specific for integrins, at the N-terminus (Figure 1B). At the C-terminus, two cysteine residues were introduced for immobilization onto a 9 nm gold

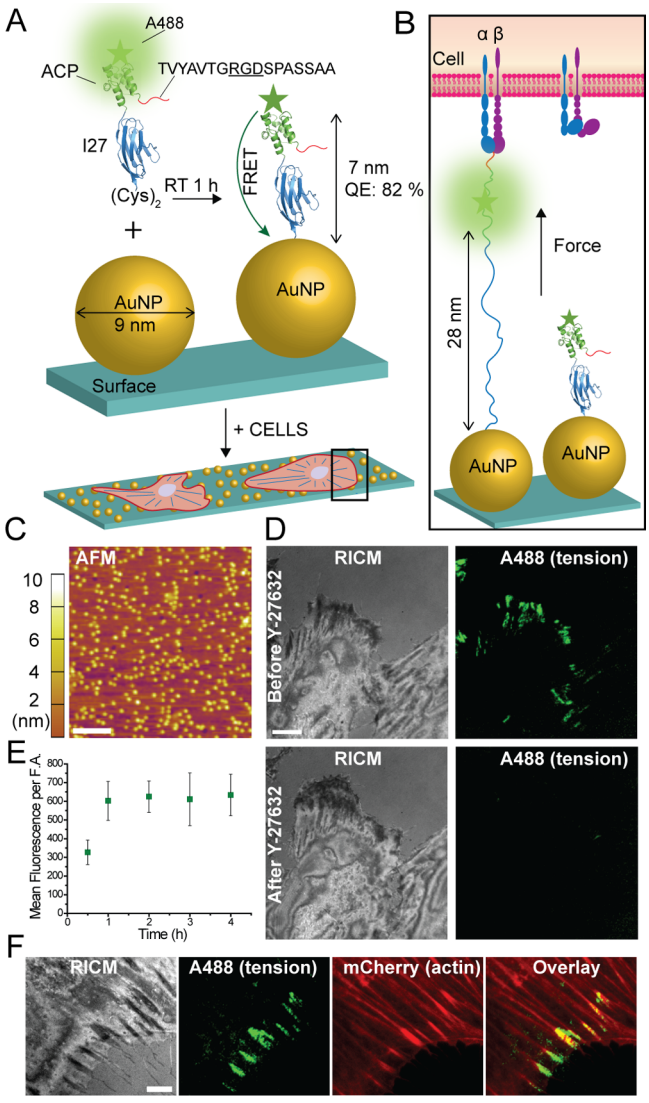

Figure 1. I27-based MTFM probes reveal integrin forces within FAs. (A−B) Schematic illustration showing the RGD-ACP(A488)-I27 probe and the mechanism of sensing (PDB ID: 1TIT and 2K92 for I27 and ACP, respectively). The probe is modified at the N terminus with FN binding motif TVYAVTGRGDSPASSAA. The C terminus included two cysteine residues for binding to the AuNP. (C) AFM image of 9 nm AuNPs immobilized on the glass coverslip. Scale bar, 200 nm. (D) Representative RICM and fluorescence images of cells incubated on the tension probe surface before and after treatment with a myosin inhibitor Y-27632 (40 μM) for 30 min. Scale bar, 10 μm. (E) Plot of the average fluorescence tension signal per FA as a function of time. The error bars represent the SEM from n = 5 cells at each time point. (F) Representative RICM and fluorescence images of REF cells that were transfected with mCherry-lifeact to visualize actin and mature focal adhesions. An overlay of the A488 channel with the mCherry channel demonstrates that integrins within FAs apply sufficient tension to unfold RGD-ACP(A488)-I27 sensor. Scale bar, 10 μm.

nanoparticle (AuNP, see AFM in Figure 1C); which serves as an efficient quencher through nanometal surface energy transfer (NSET).[12d] The RGD-ACP-I27 protein was conjugated to Alexa488, which was confirmed by SDS-PAGE and fluorescence spectrometry. UV−vis indicated a 90% labeling efficiency, and CD spectroscopy confirmed the secondary structure of the I27 construct at 37 °C (Figure S1 A−C, Supporting

DOI: 10.1021/acs.nanolett.5b03888
Nano Lett. 2016, 16, 341−348

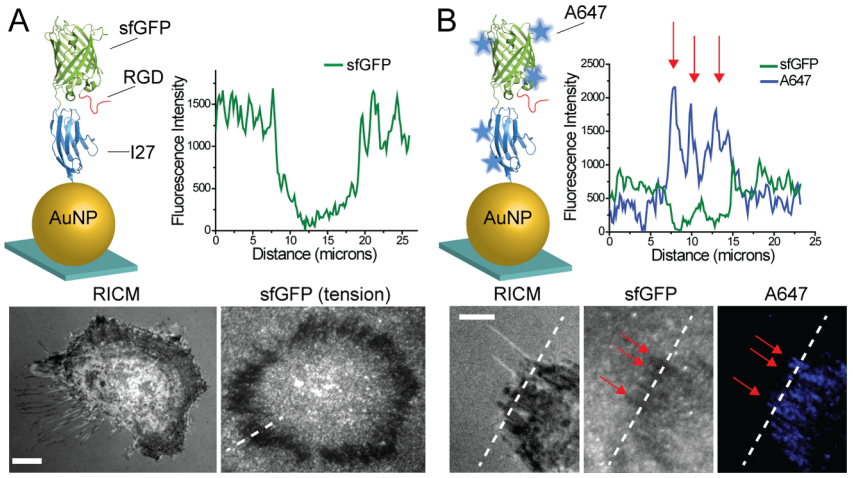

Figure 2. Integrin forces irreversibly quench and unfold sfGFP. (A) Schematic illustrating the RGD-sfGFP-I27 probe functionalized onto immobilized AuNPs (sfGFP PDB ID: 2B3P). Representative fluorescence and RICM images of REF cells cultured onto the RGD-sfGFP-I27 sensor surface for 3 h. Line scan analysis shows a loss in fluorescence at the cell edge, coinciding with the expected regions of mature FAs. (B) The RGD-sfGFP-I27 probe was nonspecifically labeled with Alexa 647, purified, and immobilized onto the AuNP surface. Representative RICM, GFP fluorescence, and Alexa 647 fluorescence images of cells incubated on the probe surface for 3 h. Line scan (dashed white line) analysis through the stress fibers (red arrows) shows anticorrelation between Alexa 647 and sfGFP emission. Scale bar, 10 μm.

Information). Protein incubation conditions were optimized to ensure that probes were specifically bound through the thiol-Au association with minimal nonspecific adsorption.[21] This required incubating the AuNP surface with a binary mixture of passivating mPEG, $SH(CH_2{-}CH_2{-}O)_8COOH$, along with the RGD-ACP(A488)-I27 probe at 1:15 molar stoichiometry for 1 h at RT. By releasing the sensor from the AuNP, we determined that each 9 nm AuNP presented an average of 5.2 sensors (Figure S1D, Supporting Information).[22] Also note that passivation was important to maintain proper orientation and function of the probe, since cells failed to engage surfaces lacking passivation with the mPEG (data not shown). With these conditions, the quenching efficiency of the ACP-tagged probes was measured at 82%, which was consistent with the dimensions of the ACP and I27 structures, and suggesting a ~7 nm fluorophore-AuNP distance.

When rat embryonic fibroblasts (REFs) were incubated on the RGD-ACP(A488)-I27 probe surface for 1 h, we observed significant signal in total internal reflection fluorescence (TIRF) that coincided with the cell edge as indicated by reflection interference contrast microscopy (RICM) (Figure 1D). The increase in fluorescence suggested that integrin-mediated forces unfolded the I27, the ACP domain, or both I27 and ACP domains, thus separating the Alexa488 reporter from the AuNP surface. To confirm that I27/ACP unfolding is driven by the cytoskeleton and specifically myosin II, we treated cells with the Rho-associated protein kinase (ROCK) inhibitor, Y-27632, for 30 min and reimaged the sample. Following ROCK inhibition, the fluorescence signal was diminished (Figure 1D) indicating that signal is reversible and mediated by myosin contractility. Further experiments show colocalization of RGD-ACP(A488)-I27 signal with the termini of F-actin stress fibers (Figure 1F). Time-lapse analysis of the tension probe signal indicated that fluorescence increased over a period of ~1 h and then held steady for at least 4 h (Figure 1E). Beyond 5 h, we typically observe a slight decrease in tension signal, likely due to a combination of thiol displacement and protease activity. The results obtained with the RGD-ACP(A488)-I27 nanoparticle probe suggest that this protein engineering strategy is suitable for investigating integrin forces, but the poorly characterized mechanical stability of ACP made it difficult to ascertain which domains mechanically unfolded.

We next incorporated superfolder green fluorescent protein (sfGFP) within the I27 MTFM probe, replacing the ACP tag. sfGFP was selected due to its mechanical stability (~100 pN unfolding force),[23] increased brightness when compared to other GFP reporters[24] and enhanced folding when fused with other proteins. The mass and fluorescence of the RGD-sfGFP-I27 construct were confirmed by SDS-PAGE and UV−vis (Figure S2 A−C, Supporting Information), and the probe was immobilized onto AuNPs as described above (Figure 2A). Surprisingly, when REF cells were cultured onto the RGD-sfGFP-I27 tension probe surface for 3 h, sfGFP emission was quenched at the perimeter of the cell (Figure 2A). Given that mechanical unfolding of GFP quenches fluorescence, we suspected that integrin-mediated forces were sufficient to unfold the β-barrel of GFP. To verify the source of sfGFP quenching, we labeled free lysine residues of the sfGFP-I27 probe with an amine-reactive Alexa647 (Figure 2B). In this case, REF cells showed an increase in Alexa647 signal that coincided with regions of sfGFP quenching. Moreover, treating cells with ROCK inhibitor did not reverse the quenched sfGFP but did lead to a decrease in Alexa647 emission (Figure S2D, Supporting Information). These experiments demonstrate that integrin-mediated forces denature and irreversibly quench sfGFP, suggesting significant tension, but it remained unclear whether I27 was stable toward integrin tension.

Unnatural amino acid incorporation was next used to express an I27 MTFM probe labeled with the *p*-azidophenylalanine amino acid. This azide-modified protein was then modified with the Cy3 dye using Cu-free click cycloaddition coupling (Figure 3A). The mass of the RGD-I27 construct was confirmed by ESI-MS; the stability of the construct at 37 °C was verified using CD spectroscopy, and the dye labeling efficiency was confirmed using SDS-PAGE and UV−vis (Figure S3 A−E, Supporting Information). Quenching efficiency upon AuNP immobilization was calculated to be 92%. This quenching efficiency roughly agreed with the predicted distance between the dye and the AuNP surface (~4 nm). Within 1 h of incubating REFs on this MTFM probe surface, we observed

DOI: 10.1021/acs.nanolett.5b03888
Nano Lett. 2016, 16, 341−348

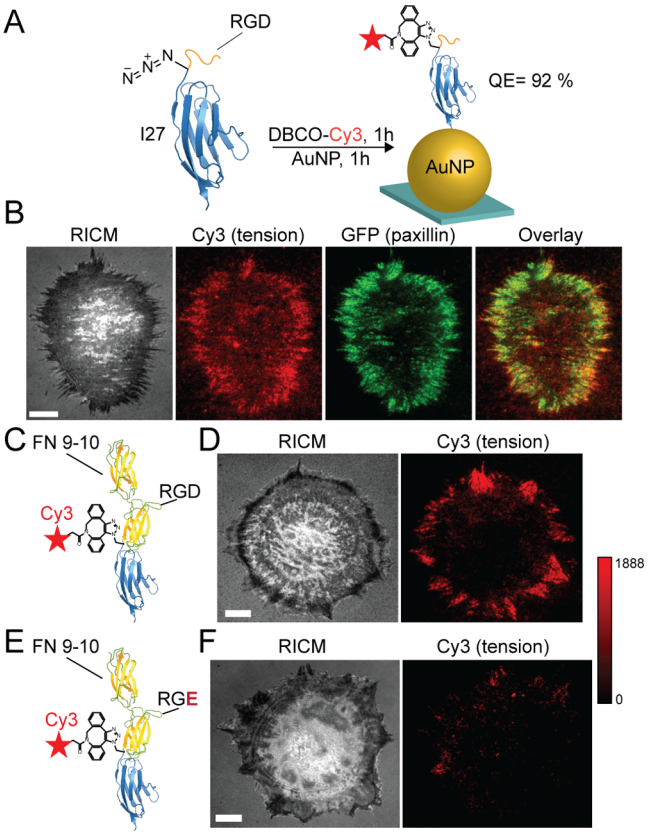

Figure 3. Integrin forces unfold I27 through RGD and FN(9−10) ligands. (A) Illustration of the RGD-Cy3-I27 MTFM sensor containing the *p*-azidophenylalanine amino acid. The dye was conjugated using Cu-free cycloaddition and was subsequently immobilized onto the AuNP surface. The quenching efficiency was 92%. (B) Representative RICM, GFP-paxillin, Cy3 tension, and overlay of Cy3/GFP shows colocalization of FAs with tension. (C) Illustration of the FN(9-10)-Cy3-I27 MTFM sensor. (D) Representative RICM and fluorescence images of REF cells that were incubated on FN(9-10)-Cy3-I27 functionalized on the AuNPs for 1 h. (E) Illustration of the FN(9-10, RGE)-I27 MTFM sensor where the highlighted point mutation is indicated in red. (F) Representative RICM and fluorescence images of REFs that were incubated on FN(9-10, RGE)-Cy3-I27 probe functionalized onto AuNPs for 1 h. The range of fluorescence intensity values for D and F are identical, and the values are displayed using the calibration bar (a.u.). Scale bar, 10 μm.

Cy3 fluorescence signal at the edges of the cell, suggesting mechanically driven I27 unfolding at these sites. Following ROCK inhibition with 40 μM of Y-27632 for 30 min, the fluorescence signal was diminished (Figure S3F, Supporting Information) showing that signal is reversible and mediated by myosin contractility. To confirm that tension signal is associated with FAs, we transfected the REFs with GFP-paxillin, a widely accepted FA marker, and found colocalization with Cy3 tension signal (Figure 3A). Importantly, this result unambiguously shows that the I27 domain is mechanically unfolded due to integrin forces within 1 h of cell adhesion.

The RGD sequence derived from FN is widely used in model cell adhesion studies.[25] However, one persistent question is whether the linear RGD sequence recapitulates the properties of more physiologically relevant ECM proteins such as domains of FN or full length FN. We rationalized that integrin-ligand binding and mechanics may be enhanced for FN domains compared to the RGD peptide fragment. To present more physiologically accurate ligands, the sensor was redesigned to present FN domains 9 and 10 at the N-terminus, providing both the synergy (PHSRN) and GRGDS motifs (Figure S4A and B, Supporting Information). Initial experiments using FN-Cy3-I27 probe showed similar spatial and temporal patterns of fluorescence as the RGD-Cy3-I27 probe (Figure 3C and D). To better understand the specificity of force transmission to the FN tension probe, we generated a control probe presenting RGE rather than the RGD sequence within the FN 10 domain (Figure 3E and F, Figure S4C, Supporting Information). In this case, we found that REF cells spread on the sensor surface but failed to generate a fluorescence response, thus suggesting that the RGD sequence within FN is required for triggering a chemo-mechanical response that generates sufficient tension to unfold I27.

Given that I27 unfolds within FAs, we infer that integrin forces range from ∼5 pN up to ∼1000 pN with the precise value depending on the loading rate and duration of the applied force. We narrowed this range of forces by measuring the initial time point of I27 unfolding following cell spreading (Supplementary Note 1). I27 probes unfold within 4 min of cell spreading over a region of interest, suggesting a minimum force of 36 pN. This value assumes an instantaneous maturation rate of FAs, which underestimates the forces applied by integrins and defines a lower estimate of integrin forces. One approach to define the upper limit of integrin tension is to challenge receptors with a probe that does not mechanically unfold. Therefore, we made use of a modified I27 which has an engineered disulfide bond buried within the core of the protein between the 32nd and 75th residues.[26] Using this reengineered I27, we generated disulfide "clamped" RGD-Cy3-$I27_{G32C\text{-}A75C}$ MTFM probe (Figure S5 A and B, Supporting Information). As illustrated in Figure 4A, the disulfide bond traps 43 amino acids (green) and leaves the other amino acids unsequestered (blue) under mechanical load. Mechanical extension of this clamped I27 stops at the disulfide bond, placing the dye at a distance of 12 nm, which is predicted to produce a QE of ∼80%. Addition of dithiothreitol (DTT) reduction agent leads to disulfide reduction and opening of the clamp. This allows for extension of the dye away from the AuNP surface to fully dequench the fluorophore. Moreover, inhibition of cell-applied force should lead to reversible refolding of I27.

In a typical experiment testing the clamped RGD-Cy3-$I27_{G32C\text{-}A75C}$, REFs were plated on the probe surface for 2 h, resulting in a weak fluorescence signal at regions that coincided with FAs (Figure 4B). This signal is likely associated with partial unfolding of I27 up to the covalent "lock". Upon addition of 0.25 mM DTT, time lapse movies showed that the signal rapidly increased, suggesting reduction of the disulfide bond and complete mechanical unfolding of the clamped probe (Figure 4B, 5A, Movie 1). To confirm that opening of the clamped sensor is myosin driven and the signal is reversible, we treated cells with the ROCK inhibitor (Y-27632) and found that the signal was diminished below the original values, prior to DTT incubation (Figure 4B and C). Control experiments indicated that pretreatment of the clamped RGD-Cy3-$I27_{G32C\text{-}A75C}$ probe with 1 mM DTT for 10 min, prior to cell plating, did not lead to increase in fluorescence and did not alter probe response following cell plating (Figure S5C, Supporting Information). Treating 50 nM of clamped RGD-Cy3-$I27_{G32C\text{-}A75C}$ probe with 10 mM DTT in solution displayed ∼10% reduction in emission (Figure S5D, Supporting

DOI: 10.1021/acs.nanolett.5b03888
Nano Lett. 2016, 16, 341−348

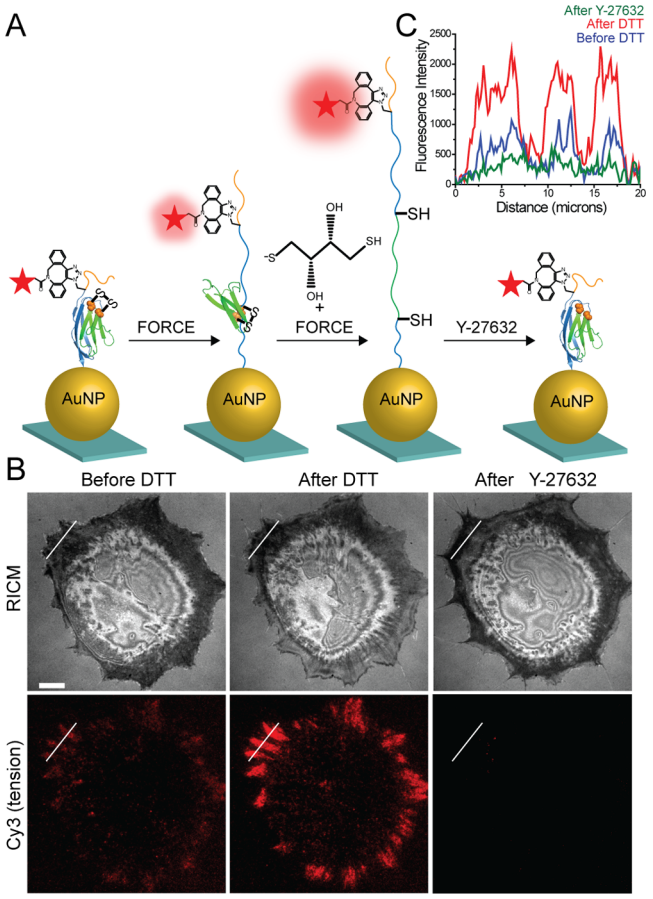

Figure 4. Covalently locked I27 resists complete mechanical unfolding by integrin forces. (A) Schematic illustration of disulfide clamped $I27_{G32C\text{-}A75C}$ tension sensor. The disulfide bridge is indicated by orange spheres. The probe was labeled with Cy3 dye and functionalized onto a AuNP surface (QE ~ 92%). When cells apply tension to the clamped MTFM sensor, I27 is stretched to the position of the disulfide clamp, resulting in solvent exposure of the disulfide. I27 can be further mechanically extended only in the presence of reducing agent, such as DTT. Refolding of the sensor is expected after ROCK kinase inhibitor (Y-27632) treatment. (B) Representative RICM and clamped I27 tension signal for REF cells incubated onto the sensor surface for 2 h before and after treatment with 0.25 mM DTT for 10 min and then after treatment with Y-27632 (40 μM) for 30 min. Scale bar, 10 μm. (C) Line scan analysis of the region of interest in B shows the fluorescence intensity through a FA before and after DTT addition and after Y-27632 treatment.

Information), whereas the probe that was immobilized to the AuNPs displayed an average of ~2% decrease in emission upon treatment with DTT. These results confirm that the buried disulfide bridge locks the I27 probe preventing mechanical unfolding, and the reduction of the disulfide bond is dependent on both the cell-applied force and the reducing agent.

Through a series of single molecule experiments,[26,27] Fernandez and co-workers found that the rate of disulfide reduction, r, for the clamped I27 was exponentially dependent on force, in accordance with the Bell model, and they showed that r was also linearly dependent on [DTT]. These relations are $r = k(F)[\mathrm{DTT}]$ and $k(F) = A\exp((F\Delta x_r - E_a)/k_BT)$, where A is a pre-exponential factor, Δx_r is the distance to the transition state of the reaction, and E_a is activation energy for the disulfide bond reduction. By varying the force and [DTT], and measuring r, Fernandez and co-workers determined Δx_r, A, and E_a for mechanically catalyzed disulfide reduction in I27. By using these validated constants for I27, we next inferred the magnitude of force experienced by the I27 probe by recording the rate of disulfide reduction as determined from the rate of fluorescence increase (Figure S6, Supporting Information). Although Δx_r, A, and E_a were determined in three reports using different mechanical loading conditions (see SI table),[27a,d,28] we used fitting values of $A = 1.3 \times 10^{12}$ M^{-1} s^{-1}, $\Delta x_r = 0.34$ Å, and $E_a = 65$ kJ from the most relevant study where $k(F)$ was determined by varying DTT concentration.[27a]

We recorded the rate of fluorescence increase for cells treated with DTT concentrations ranging from 0.25 mM up to 25 mM (Figure 5B; $n = 25$ cells total) at varying sampling frequencies in order to collect enough data points to obtain an accurate fit of the kinetic curves (SI methods). By fitting the increase of fluorescence versus time, we measured the time constant of disulfide reduction, τ_r, and thus determined the rate of disulfide reduction ($r = 1/\tau_r$) from cell experiments. DTT concentrations greater than 25 mM induced a reduction in cell adhesion, suggesting cell toxicity, which is confirmed by literature studying the effect of DTT on redox signaling in fibroblasts.[29] In contrast, treating REFs expressing GFP-β_3 with 2.5 mM DTT for 10 min did not lead to any observable change in cell morphology or GFP signal (Figure S5E, Supporting Information). To show the spatial heterogeneity of disulfide reduction rates within a single cell, we generated a heat map of rates (ranging from 0.005 to 0.05 s^{-1}) using the programming software (IDL, Figure 5C). As the heat map suggests, there is significant heterogeneity of r values within a single cell. Upon closer inspection of r values within FAs and overlaying of the final tension signal against r, we were not able to identify a correlation between the intensity of the tension signal and the rate of thiol exchange. We next plotted the average r for different DTT concentrations (Figure 5D) and then determined $k(F)$ from the slope of this plot (Figure S6, Supporting Information). Assuming that the integrin force is constant within the time window of observation (<4 min) with minimal receptor turnover, we estimate that unfolded tension probes experience an average of 110 ± 9 pN (Figure S6, Supporting Information). This assumption is supported by literature showing more stable FA dynamics after 1.5 h of REF cell adhesion.[30] Furthermore, the tension signal appears static after the signal saturates reaching maximal thiol exchange, thus suggesting that there is limited FA turnover after cells are allowed to fully adhere on the surface. This value suggests that a subset of integrins experience forces that have been significantly underestimated.

To investigate force dependence on integrin subtype, we treated the cells with blocking antibodies against $\alpha_v\beta_3$ and $\alpha_5\beta_1$ and repeated the kinetic measurements described above. The efficiency of antibody blocking was confirmed by using GFP-β_3 expressing cells (Figure S7A, Supporting Information). Blocking with both antibodies abrogated cell adhesion, indicating that these two integrins are the primary receptors mediating cell adhesion (Figure S7B, Supporting Information). Cells primarily using $\alpha_v\beta_3$ integrins displayed slowed rates of disulfide reduction indicating a tension of 40 ± 7 pN. This is in contrast to cells employing $\alpha_5\beta_1$ integrins, which showed accelerated rates of disulfide reduction with average forces of 160 ± 7 pN. These values are consistent with precedent indicating greater rupture forces for $\alpha_5\beta_1$ compared to $\alpha_v\beta_3$.[31]

There is disagreement in the literature regarding the magnitude of integrin-ligand tension within FAs. Dunn and

DOI: 10.1021/acs.nanolett.5b03888
Nano Lett. 2016, 16, 341−348

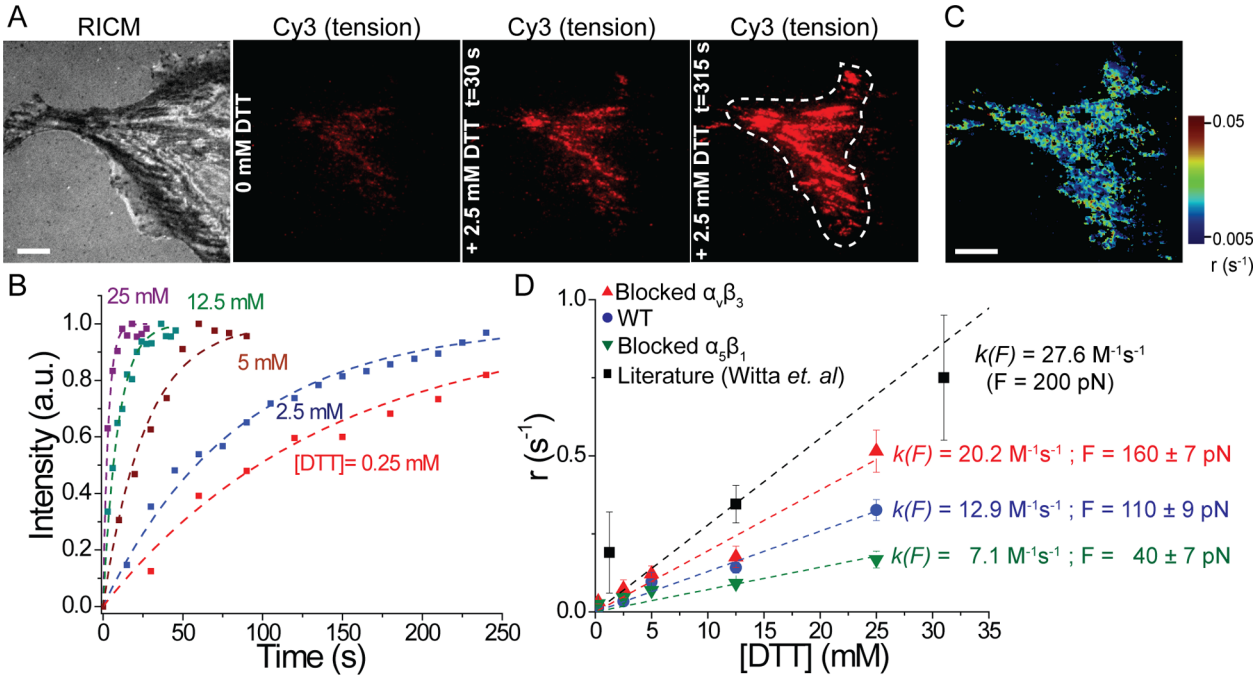

Figure 5. Kinetic measurements of S−S reduction to determine integrin forces. (A) Representative RICM and fluorescence images of clamped $I27_{G32C\text{-}A75C}$ sensor before and after DTT addition at t = 30 and 315 s. White dashed line shows the region of interest that was analyzed. Scale bar, 10 μm. (B) Representative kinetic plots showing an increase in fluorescence tension signal at different DTT concentrations. Dashed lines represent single-exponential fits used to determine τ_r. (C) Heat map of disulfide reduction rates generated from the fluorescence video of the cell depicted in A. Scale bar, 10 μm. (D) Plot of the rate of disulfide reduction ($r = 1/\tau_r$) as a function of [DTT] for REF cells (blue), REF cells blocked with $\alpha v\beta 3$ (red), and $\alpha 5\beta 1$ antibodies (green). $k(F)$ and F were derived from the linear fit of each data set. Black squares and fit (dashed line) are from Witta et al. *PNAS*, **2006** where clamped I27 was subjected to a constant force of 200 pN, which generated a slope of 27.6 M^{-1} s^{-1}. This previous work included DTT concentration up to 125 mM, but the additional data points were omitted for clarity. Error bars represent the SEM of r obtained from n = 5 cells at each concentration of DTT (0.5 mM, 2.5 mM, 5 mM, 12.5 mM, and 25 mM).

colleagues suggest an integrin-ligand force of 1−5 pN in human foreskin fibroblasts by using single molecule FRET.[14a] In agreement with this estimate, Schwartz et al. calculate cell traction forces of a few pN per integrin receptor in mouse embryo fibroblasts by averaging cell stress over the average number of integrins per unit area.[9a] In contrast, we previously inferred greater integrin forces >20 pN per receptor based on the observation of mechanically induced biotin−streptavidin dissociation in many cell types.[12f] The tension gauge tether (TGT) technique also suggests greater integrin forces and a peak force of 56 pN for integrin activation.[7]

The I27 tension probes are more mechanically robust than any other sensor tested to date, thus investigating a greater range of integrin tension values. Except for the disulfide clamped RGD-Cy3-$I27_{G32C\text{-}A75C}$, all probes (RGD-ACP(A488)-I27, RGD-sfGFP-I27, RGD-Cy3-I27, FN-A647-I27) were mechanically unfolded by integrin forces displaying a fluorescence response. The sfGFP probe showed mechanically induced quenching which has been investigated by theory and experiments[32] and is thought to require ∼100−200 pN (using a 300 nm/s loading rate).[23a] This surprising result indicates that genetically encoded tension probes for cell adhesion proteins are susceptible to mechanical quenching. For example, genetically encoding an integrin tension probe akin to the vinculin tension sensor[8] is not likely to succeed. Although I27 is a highly reversible folder, sfGFP does not recover its full fluorescence after refolding, which may explain why treating cells with the ROCK inhibitor did not lead to full recovery of sfGFP fluorescence.

Importantly, using equilibrium distribution of folded to unfolded tension probes to estimate integrin forces is limited for the following reasons: (a) mechanical unfolding is highly dependent on the duration of force (Supplementary Note 1), which is unknown because FA maturation is heterogeneous, (b) mechanical unfolding is dependent on the loading rate, which is also unknown during FA maturation, and (c) once the applied forces cause unfolding, this defines a minimum tension but not the average tension. Using single molecule techniques can, in principle, overcome the challenges of ensemble averaging to estimate the tension for each receptor. However, single molecule imaging produces a sparse density of reporters since only one receptor is characterized within an area of ∼2 μm^2 and there are hundreds of integrin receptors within such an area.[14a] We overcome these limitations by recording the rate of disulfide reduction. Note that a fundamental assumption for force estimates determined by using the kinetics of disulfide reduction are the reaction parameters measured by Fernandez and colleagues. Any significant errors in those measurements will lead to significant deviations in our reported values. Nonetheless, these parameters have been validated in a number of papers.[26,27]

By blocking REFs with monoclonal antibodies against $\alpha_v\beta_3$ and $\alpha_5\beta_1$, we showed that the cell-generated forces are integrin-subtype dependent. The rate of I27 unfolding by $\alpha_v\beta_3$ integrin is 3-fold smaller than that for the $\alpha_5\beta_1$ integrins. The mechanism behind differential force levels for different integrin subtypes is likely due to the different functions of each integrin within cell-ECM adhesions. During cell migration, force sensing at the cell edge requires constant recycling of $\alpha_v\beta_3$ integrins that

DOI: 10.1021/acs.nanolett.5b03888
Nano Lett. 2016, 16, 341−348

promotes mechanotransduction and reinforcement of other integrins and proteins to the sites of adhesions.[33] However, cells dampen migration by engaging more $\alpha_5\beta_1$ integrins and by generating stable adhesion sites that require stronger integrin-ligand bonds to resist high forces. Sheetz et al. found that clustering of $\alpha_5\beta_1$ integrins enhances rupture forces by 6-fold compared to the $\alpha_v\beta_3$ integrins.[31] This is consistent with our results.

High magnitude forces reported through the I27 probe likely pertain to a small subset of force bearing receptors. This is consistent with the conclusion that the average integrin tension within FAs is 2−4 pN as determined by TFM.[9a] Also DNA- and PEG-based MTFM probes sensitive to ∼1−20 pN forces generate signal more rapidly following cell plating. Therefore, the results reveal the existence of "hot" receptors that carry a greater fraction of cell traction forces. High magnitude integrin forces exist with FN and RGD ligands as both types of I27 probes display similar signal. Future experiments with multiplexed tension probes will generate a more comprehensive histogram of integrin force distributions within FAs.

In summary, we report a new class of I27-based tension probes that provides many advantages over the previously reported MTFM probes. First, I27 tension probes are mechanically responsive to greater magnitude of forces, and, in principle, the response threshold can range from ∼40 pN to ∼100 pN by inserting point mutations within the I27 domain. This feature significantly expands the current range of forces detected by MTFM probes. Second, the disulfide bridge clamped sensor circumvents caveats inherent to the transient nature of focal adhesion maturation and the loading rate dependence of mechanical extension, which is a long-standing issue with FRET-based tension sensors. Last, I27-based protein sensors can be easily engineered to incorporate virtually any recombinant protein ligand which provides a general approach that can be adapted for the study of a wide range of mechanotransduction processes.

■ ASSOCIATED CONTENT

Supporting Information

The Supporting Information is available free of charge on the ACS Publications website at DOI: 10.1021/acs.nanolett.5b03888.

Materials and methods and additional figures (PDF)
Quantification of integrin tension for REF cells (AVI)

■ AUTHOR INFORMATION

Corresponding Author

*E-mail: k.salaita@emory.edu.

Author Contributions

K.G. and Y.L. contributed equally.

Notes

The authors declare no competing financial interest.

■ ACKNOWLEDGMENTS

We thank Dr. Oskar Laur from Custom Cloning Core Facility Yerkes-Microbiology at Emory University for sequencing all the plasmids. We thank Leann Quertinmont (Emory University) for DH5-alpha and BL21(DE3) competent *E. coli* cells. We thank Dr. Benjamin Geiger (Department of Molecular Cell Biology at Weizmann Institute) for REF cells stably expressing GFP-tagged β3-integrins. We also thank Dr. Ada Cavalcanti-Adam (Max Planck Institute for Intelligent Systems, Stuttgart, Germany) for plasmid encoding mCherry-lifeact. K.S. acknowledges support from the NIH (R01-GM097399), the Alfred P. Sloan Research Fellowship, and the NSF CAREER award.

■ REFERENCES

(1) Hynes, R. O. Integrins: bidirectional, allosteric signaling machines. *Cell* **2002**, *110* (6), 673−87.

(2) Redick, S. D.; Settles, D. L.; Briscoe, G.; Erickson, H. P. Defining fibronectin's cell adhesion synergy site by site-directed mutagenesis. *J. Cell Biol.* **2000**, *149* (2), 521−527.

(3) Barczyk, M.; Carracedo, S.; Gullberg, D. Integrins. *Cell Tissue Res.* **2010**, *339* (1), 269−80.

(4) Humphrey, J. D.; Dufresne, E. R.; Schwartz, M. A. Mechanotransduction and extracellular matrix homeostasis. *Nat. Rev. Mol. Cell Biol.* **2014**, *15* (12), 802−12.

(5) Kanchanawong, P.; Shtengel, G.; Pasapera, A. M.; Ramko, E. B.; Davidson, M. W.; Hess, H. F.; Waterman, C. M. Nanoscale architecture of integrin-based cell adhesions. *Nature* **2010**, *468* (7323), 580−4.

(6) (a) Parsons, J. T.; Horwitz, A. R.; Schwartz, M. A. Cell adhesion: integrating cytoskeletal dynamics and cellular tension. *Nat. Rev. Mol. Cell Biol.* **2010**, *11* (9), 633−43. (b) Liu, Z.; Liu, Y.; Chang, Y.; Seyf, H. R.; Henry, A.; Mattheyses, A. L.; Yehl, K.; Zhang, Y.; Huang, Z.; Salaita, K. *Nat. Meth.* **2015**, in press.

(7) Wang, X.; Ha, T. Defining single molecular forces required to activate integrin and notch signaling. *Science* **2013**, *340* (6135), 991−4.

(8) Grashoff, C.; Hoffman, B. D.; Brenner, M. D.; Zhou, R.; Parsons, M.; Yang, M. T.; McLean, M. A.; Sligar, S. G.; Chen, C. S.; Ha, T.; Schwartz, M. A. Measuring mechanical tension across vinculin reveals regulation of focal adhesion dynamics. *Nature* **2010**, *466* (7303), 263−6.

(9) (a) Sabass, B.; Gardel, M. L.; Waterman, C. M.; Schwarz, U. S. High resolution traction force microscopy based on experimental and computational advances. *Biophys. J.* **2008**, *94* (1), 207−20. (b) Tan, J. L.; Tien, J.; Pirone, D. M.; Gray, D. S.; Bhadriraju, K.; Chen, C. S. Cells lying on a bed of microneedles: an approach to isolate mechanical force. *Proc. Natl. Acad. Sci. U. S. A.* **2003**, *100* (4), 1484−9.

(10) Wiseman, P. W.; Brown, C. M.; Webb, D. J.; Hebert, B.; Johnson, N. L.; Squier, J. A.; Ellisman, M. H.; Horwitz, A. F. Spatial mapping of integrin interactions and dynamics during cell migration by image correlation microscopy. *J. Cell Sci.* **2004**, *117* (23), 5521−5534.

(11) Engler, A. J.; Sen, S.; Sweeney, H. L.; Discher, D. E. Matrix elasticity directs stem cell lineage specification. *Cell* **2006**, *126* (4), 677−89.

(12) (a) Stabley, D. R.; Jurchenko, C.; Marshall, S. S.; Salaita, K. S. Visualizing mechanical tension across membrane receptors with a fluorescent sensor. *Nat. Methods* **2011**, *9* (1), 64−67. (b) Jurchenko, C.; Salaita, K. S. Lighting up the Force: Investigating Mechanisms of Mechanotransduction Using Fluorescent Tension Probes. *Mol. Cell. Biol.* **2015**, *35*, 2570. (c) Zhang, Y.; Ge, C.; Zhu, C.; Salaita, K. DNA-based digital tension probes reveal integrin forces during early cell adhesion. *Nat. Commun.* **2014**, *5*, 5167. (d) Liu, Y.; Medda, R.; Liu, Z.; Galior, K.; Yehl, K.; Spatz, J. P.; Cavalcanti-Adam, E. A.; Salaita, K. Nanoparticle tension probes patterned at the nanoscale: impact of integrin clustering on force transmission. *Nano Lett.* **2014**, *14* (10), 5539−46. (e) Liu, Y.; Yehl, K.; Narui, Y.; Salaita, K. Tension sensing nanoparticles for mechano-imaging at the living/nonliving interface. *J. Am. Chem. Soc.* **2013**, *135* (14), 5320−3. (f) Jurchenko, C.; Chang, Y.; Narui, Y.; Zhang, Y.; Salaita, K. S. Integrin-generated forces lead to streptavidin-biotin unbinding in cellular adhesions. *Biophys. J.* **2014**, *106* (7), 1436−46.

(13) Blakely, B. L.; Dumelin, C. E.; Trappmann, B.; McGregor, L. M.; Choi, C. K.; Anthony, P. C.; Duesterberg, V. K.; Baker, B. M.; Block, S. M.; Liu, D. R.; Chen, C. S. A DNA-based molecular probe for optically reporting cellular traction forces. *Nat. Methods* **2014**, *11* (12), 1229−32.

DOI: 10.1021/acs.nanolett.5b03888
Nano Lett. 2016, 16, 341−348

(14) (a) Morimatsu, M.; Mekhdjian, A. H.; Adhikari, A. S.; Dunn, A. R. Molecular tension sensors report forces generated by single integrin molecules in living cells. *Nano Lett.* **2013**, *13* (9), 3985−9. (b) Morimatsu, M.; Mekhdjian, A. H.; Chang, A. C.; Tan, S. J.; Dunn, A. R. Visualizing the interior architecture of focal adhesions with high-resolution traction maps. *Nano Lett.* **2015**, *15* (4), 2220−8.
(15) Botello, E.; Harris, N. C.; Sargent, J.; Chen, W. H.; Lin, K. J.; Kiang, C. H. Temperature and chemical denaturant dependence of forced unfolding of titin I27. *J. Phys. Chem. B* **2009**, *113* (31), 10845−8.
(16) Lu, H.; Isralewitz, B.; Krammer, A.; Vogel, V.; Schulten, K. Unfolding of titin immunoglobulin domains by steered molecular dynamics simulation. *Biophys. J.* **1998**, *75* (2), 662−71.
(17) Rief, M.; Gautel, M.; Oesterhelt, F.; Fernandez, J. M.; Gaub, H. E. Reversible unfolding of individual titin immunoglobulin domains by AFM. *Science* **1997**, *276* (5315), 1109−12.
(18) Li, H.; Carrion-Vazquez, M.; Oberhauser, A. F.; Marszalek, P. E.; Fernandez, J. M. Point mutations alter the mechanical stability of immunoglobulin modules. *Nat. Struct. Biol.* **2000**, *7* (12), 1117−1120.
(19) Szoszkiewicz, R.; Ainavarapu, S. R.; Wiita, A. P.; Perez-Jimenez, R.; Sanchez-Ruiz, J. M.; Fernandez, J. M. Dwell time analysis of a single-molecule mechanochemical reaction. *Langmuir* **2008**, *24* (4), 1356−64.
(20) Zhou, Z.; Cironi, P.; Lin, A. J.; Xu, Y.; Hrvatin, S.; Golan, D. E.; Silver, P. A.; Walsh, C. T.; Yin, J. Genetically encoded short peptide tags for orthogonal protein labeling by Sfp and AcpS phosphopantetheinyl transferases. *ACS Chem. Biol.* **2007**, *2* (5), 337−46.
(21) Aubin-Tam, M. E. Conjugation of nanoparticles to proteins. *Methods Mol. Biol.* **2013**, *1025*, 19−27.
(22) (a) Yehl, K.; Joshi, J. P.; Greene, B. L.; Dyer, R. B.; Nahta, R.; Salaita, K. Catalytic deoxyribozyme-modified nanoparticles for RNAi-independent gene regulation. *ACS Nano* **2012**, *6* (10), 9150−7. (b) Yehl, K.; Mugler, A.; Vivek, S.; Liu, Y.; Zhang, Y.; Fan, M.; Weeks, E. R.; Salaita, K. High-speed DNA-based rolling motors powered by RNase H. *Nat. Nanotechnol.* **2015**, in press.
(23) (a) Dietz, H.; Rief, M. Exploring the energy landscape of GFP by single-molecule mechanical experiments. *Proc. Natl. Acad. Sci. U. S. A.* **2004**, *101* (46), 16192−7. (b) Otten, M.; Ott, W.; Jobst, M. A.; Milles, L. F.; Verdorfer, T.; Pippig, D. A.; Nash, M. A.; Gaub, H. E. From genes to protein mechanics on a chip. *Nat. Methods* **2014**, *11* (11), 1127−30.
(24) Pedelacq, J. D.; Cabantous, S.; Tran, T.; Terwilliger, T. C.; Waldo, G. S. Engineering and characterization of a superfolder green fluorescent protein. *Nat. Biotechnol.* **2006**, *24* (1), 79−88.
(25) Pankov, R.; Yamada, K. M. Fibronectin at a glance. *J. Cell Sci.* **2002**, *115* (20), 3861−3863.
(26) Ainavarapu, S. R.; Brujic, J.; Huang, H. H.; Wiita, A. P.; Lu, H.; Li, L.; Walther, K. A.; Carrion-Vazquez, M.; Li, H.; Fernandez, J. M. Contour length and refolding rate of a small protein controlled by engineered disulfide bonds. *Biophys. J.* **2007**, *92* (1), 225−33.
(27) (a) Wiita, A. P.; Ainavarapu, S. R.; Huang, H. H.; Fernandez, J. M. Force-dependent chemical kinetics of disulfide bond reduction observed with single-molecule techniques. *Proc. Natl. Acad. Sci. U. S. A.* **2006**, *103* (19), 7222−7. (b) Ainavarapu, S. R.; Wiita, A. P.; Huang, H. H.; Fernandez, J. M. A single-molecule assay to directly identify solvent-accessible disulfide bonds and probe their effect on protein folding. *J. Am. Chem. Soc.* **2008**, *130* (2), 436−7. (c) Wiita, A. P.; Perez-Jimenez, R.; Walther, K. A.; Grater, F.; Berne, B. J.; Holmgren, A.; Sanchez-Ruiz, J. M.; Fernandez, J. M. Probing the chemistry of thioredoxin catalysis with force. *Nature* **2007**, *450* (7166), 124−7. (d) Liang, J.; Fernandez, J. M. Kinetic measurements on single-molecule disulfide bond cleavage. *J. Am. Chem. Soc.* **2011**, *133* (10), 3528−34.
(28) Koti Ainavarapu, S. R.; Wiita, A. P.; Dougan, L.; Uggerud, E.; Fernandez, J. M. Single-molecule force spectroscopy measurements of bond elongation during a bimolecular reaction. *J. Am. Chem. Soc.* **2008**, *130* (20), 6479−87.
(29) Pani, G.; Colavitti, R.; Bedogni, B.; Anzevino, R.; Borrello, S.; Galeotti, T. A redox signaling mechanism for density-dependent inhibition of cell growth. *J. Biol. Chem.* **2000**, *275* (49), 38891−9.
(30) Aroush, D.; Zaidel-Bar, R.; Bershadsky, A. D.; Wagner, H. D. Temporal evolution of cell focal adhesions: experimental observations and shear stress profiles. *Soft Matter* **2008**, *4* (12), 2410−2417.
(31) Roca-Cusachs, P.; Gauthier, N. C.; Del Rio, A.; Sheetz, M. P. Clustering of alpha(5)beta(1) integrins determines adhesion strength whereas alpha(v)beta(3) and talin enable mechanotransduction. *Proc. Natl. Acad. Sci. U. S. A.* **2009**, *106* (38), 16245−50.
(32) Saeger, J.; Hytonen, V. P.; Klotzsch, E.; Vogel, V. GFP's mechanical intermediate states. *PLoS One* **2012**, *7* (10), e46962.
(33) White, D. P.; Caswell, P. T.; Norman, J. C. alpha v beta3 and alpha5beta1 integrin recycling pathways dictate downstream Rho kinase signaling to regulate persistent cell migration. *J. Cell Biol.* **2007**, *177* (3), 515−25.

DOI: 10.1021/acs.nanolett.5b03888
Nano Lett. 2016, 16, 341−348